A Nonlinear Hybrid Vortex Method for Wings at Large Angle of Attack

Osama A. Kandil,* Li-Chuan Chu,† and Thomas Tureaud‡
Old Dominion University, Norfolk, Virginia

A steady and unsteady nonlinear hybrid vortex (NHV) method is developed for low aspect ratio wings at large angles of attack. The method uses vortex panels with linear vorticity distribution (equivalent to a quadratic doublet distribution) to calculate the induced velocity in the near field using closed-form expressions. In the far field, the distributed vorticity is reduced to concentrated vortex lines and the simpler Biot-Savart law is employed. The method is applied to rectangular wings in steady and unsteady flows. The numerical results show that the method accurately predicts the distributed aerodynamic loads and that it is of acceptable computational efficiency.

I. Introduction and Background

In recent years, the development of numerical methods for predicting the steady and unsteady aerodynamic characteristics of lifting surfaces exhibiting leading- and/or side-edge separations has received considerable attention.

For the steady flow problems several numerical techniques have been developed. These include the nonlinear discrete vortex[1-6] (NDV) methods, higher order doublet panel methods,[7-9] and nonlinear hybrid vortex (NHV) methods.[10,11] For the unsteady flow problems, the literature shows fewer numerical techniques which include the NDV methods[12-15] and constant doublet panel methods.[16,17] The literature lacks high-order panel methods for the unsteady flow problems.

For this reason, we are presenting in this paper an efficient and accurate method for the steady and unsteady flow problems of lifting surfaces at large angles of attack.

In this method, vortex panels with linear vorticity distribution are used in the near field calculations. In the far-field calculations, the distributed vorticity over each far-field panel is lumped into equivalent concentrated vortex lines. In this way, accuracy is satisfied in the near field while computational efficiency is maintained in the far field. The coupling of a continuous vortex-sheet representation and a concentrated vortex-line representation for solving the nonlinear lifting surface problem is called the "nonlinear hybrid vortex" (NHV) method.

II. Formulation of the Problem

The problem is formulated relative to a wing-fixed frame of reference xyz. The x axis is the wing centerline and the xy plane is the wing plane of symmetry. The wing is rotating at the angular velocity $\bar{\Omega}$ and the freestream velocity is $\bar{U}_\infty$. The general orientation of the wing is described using the Eulerian angles α, β, and γ (Fig. 1), which refer to the angles of attack, yaw, and roll, respectively. In terms of these angles and their time rate of change, the dimensionless freestream velocity and the angular velocity are expressed by

$$\bar{e}_\infty = \cos\alpha\cos\beta\,\bar{i} + (-\sin\alpha\cos\gamma + \cos\alpha\sin\beta\sin\gamma)\bar{j} + (\sin\alpha\sin\gamma + \cos\alpha\sin\beta\cos\gamma)\bar{k} \tag{1}$$

$$\bar{\Omega} = (-\dot{\alpha}\sin\beta + \dot{\gamma})\bar{i} + (\dot{\alpha}\cos\beta\sin\gamma + \dot{\beta}\cos\gamma)\bar{j} + (\dot{\alpha}\cos\beta\cos\gamma - \dot{\beta}\sin\gamma)\bar{k} = \Omega_x\bar{i} + \Omega_y\bar{j} + \Omega_z\bar{k} \tag{2}$$

where $\bar{i}$, $\bar{j}$, and $\bar{k}$ are the base unit vectors of the xyz frame of reference.

The unsteady irrotational ideal flow in the region outside of the wing and its separated vortex sheets is governed by the Laplace equation

$$\nabla^2\phi = 0 \tag{3}$$

where $\phi(\bar{r},t)$ is the perturbation velocity potential. The no-penetration condition on the wing $s(\bar{r},t)$, relative to the wing fixed frame of reference, is given by

$$\partial s/\partial t + (\bar{e}_\infty + \nabla\phi - \bar{\Omega}\times\bar{r})\cdot\nabla s = 0 \qquad \text{on } s(\bar{r},t) = 0 \tag{4a}$$

For a rigid wing, $\partial s/\partial t = 0$ and Eq. (4a) reduces to

$$(\bar{e}_\infty + \nabla\phi - \bar{\Omega}\times\bar{r})\cdot\bar{n}_s = 0 \qquad \text{on } s(\bar{r}) = 0 \tag{4b}$$

On the separated free-vortex sheet $w(\bar{r},t)$, the no-penetration condition is given by

$$\partial w/\partial t + (\bar{e}_\infty + \nabla\phi - \bar{\Omega}\times\bar{r})\cdot\nabla w = 0 \qquad \text{on } w(\bar{r},t) = 0 \tag{5}$$

The no-pressure jump condition on $w(\bar{r},t)$ is obtained from the unsteady incompressible Bernoulli equation

$$C_p(\bar{r},t) = -\nabla\phi\cdot[\nabla\phi + 2(\bar{e}_\infty - \bar{\Omega}\times\bar{r})] - 2(\partial\phi/\partial t) \tag{5a}$$

where $C_p(\bar{r},t)$ is the pressure coefficient at any point $\bar{r}$ and at any time t. Forming the pressure jump from Eq. (5a) and equating the result to zero, we obtain

$$\Delta C_p = C_{p1} - C_{p2} = -(\nabla\phi_1 - \nabla\phi_2)\cdot[\nabla\phi_1 + \nabla\phi_2 + 2(\bar{e}_\infty - \bar{\Omega}\times\bar{r})] - 2\frac{\partial}{\partial t}(\phi_1 - \phi_2) = 0 \tag{5b}$$

where subscripts *1* and *2* refer to the upper and lower surfaces of the wing, respectively. Rearranging Eq. (5b) and setting

$$\phi_1 - \phi_2 = \Delta\phi \tag{5c}$$

Presented at Paper 82-0351 at the AIAA 20th Aerospace Sciences Meeting, Orlando, Fla., Jan. 11-14, 1982; submitted March 1, 1982; revision received March 7, 1983.

*Associate Professor of Mechanical Engineering and Mechanics. Member AIAA.

†Graduate Research Assistant. Member AIAA.

one obtains

$$\Delta C_p = -2\left(\frac{\partial}{\partial t} + \bar{v}_w \cdot \nabla\right)(\Delta\phi) = -2\frac{\mathrm{D}}{\mathrm{D}t}(\Delta\phi) = 0 \qquad (5d)$$

where $\bar{v}_w$ is the velocity of a wake element relative to the xyz frame of reference

$$\bar{v}_w = \tfrac{1}{2}(\nabla\phi_1 + \nabla\phi_2) + \bar{e}_\infty - \bar{\Omega}\times\bar{r}$$

Equation (5d) represents the theorems of Kelvin and Helmholtz

$$\frac{\mathrm{D}\Gamma}{\mathrm{D}t} = \frac{\mathrm{D}}{\mathrm{D}t}\iint \bar{\omega}\cdot\bar{n}_A \mathrm{d}A = 0 \quad \text{on } w(\bar{r},t) = 0 \qquad (6)$$

of conservation of the circulation and the outflow of vorticity, respectively. In Eq. (6), $\bar{n}_A$ is a unit normal to the surface A bounded by a closed curve around which the circulation Γ is calculated. Equation (6) simply states that the rate of change of circulation around a closed curve or the rate of change of outflow of vorticity through the surface bounded by this closed curve is zero (following the same fluid particles).

For uniqueness of the solution one has to impose the Kutta condition along the edges of separation. Here, the Kutta conditon is represented by

$$\Delta C_p \Big|_{\text{TE,LE,SE}} = 0 \qquad (7)$$

Finally, the infinity condition requires that

$$\nabla\phi \to 0 \text{ away from } s \text{ and } w \qquad (8)$$

Equations (1-8) are the required equations for the general unsteady flow problem.

III. Nonlinear Hybrid-Vortex Method for Steady Flows

A. Governing Equations

The research effort in this paper is concentrated on the symmetric flow problems. For a steady symmetric flow, the governing equations are obtained from the general equations (1-8) by setting $\bar{\Omega}=0$, $\beta=\gamma=0$, and dropping the time-dependent terms.

$$\bar{e}_\infty = \cos\alpha\,\bar{i} - \sin\alpha\,\bar{j} \qquad (9)$$

$$\nabla^2\phi = 0 \qquad (10)$$

$$(\bar{e}_\infty + \nabla\phi)\cdot\bar{n}_s = 0 \quad \text{on } s(\bar{r}) = 0 \qquad (11)$$

$$(\bar{e}_\infty + \nabla\phi)\cdot\bar{n}_w = 0 \quad \text{on } w(\bar{r}) = 0 \qquad (12)$$

$$\Delta C_p = -2(\bar{n}_w \times \bar{\omega})\cdot(\bar{e}_\infty + \nabla\phi) = 0 \quad \text{on } w(\bar{r}) = 0 \qquad (13)$$

$$\Delta C_p \Big|_{\text{TE,LE,SE}} = 0 \qquad (14)$$

$$\nabla\phi \to 0 \quad \text{away from } s \text{ and } w \qquad (15)$$

B. Method of Solution of the Steady Flow Problem

Equation (12) requires the flow to be tangent to w while Eq. (13) requires this tangential flow to be parallel to the vorticity direction. Therefore, if the position of w is adjusted so that the flow direction is parallel to the vorticity direction on the surface w, the boundary conditions of Eq. (12) and (13) are automatically satisfied. Next, we outline the method of solution.

Once the wing and its free-shear layers are represented by vortex sheets, Eqs. (10) and (15) are automatically satisfied. The basic unknowns in the present problem are the vorticity distribution $\bar{\omega}$ fand the free-vortex sheet w. They are determined by satisfying the remaining boundary conditions, Eqs. (11-14), through a "panel method."

In this method, the bound-vortex sheet (representing the wing) is divided into quadrilateral bound-vortex panels, while the free-vortex sheets (representing the free-shear layers) are divided into triangular free-vortex panels (see Fig. 2). On each vortex panel (bound or free), a local vorticity distribution with undetermined coefficients is defined in a local coordinate system. The local distribution is selected such that the solenoidal property of vorticity is satisfied. The continuity of vorticity (a compatibility condition) is enforced at certain nodes (defined later) on the interelement boundaries of adjacent panels.

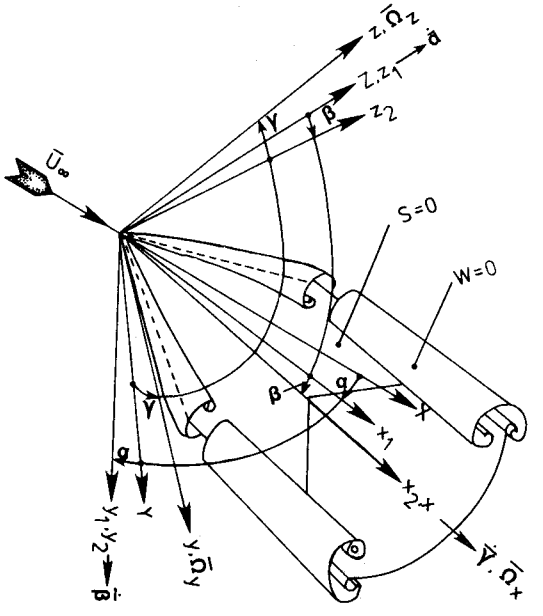

Fig. 1 Frames of reference and Eulerian's angles.

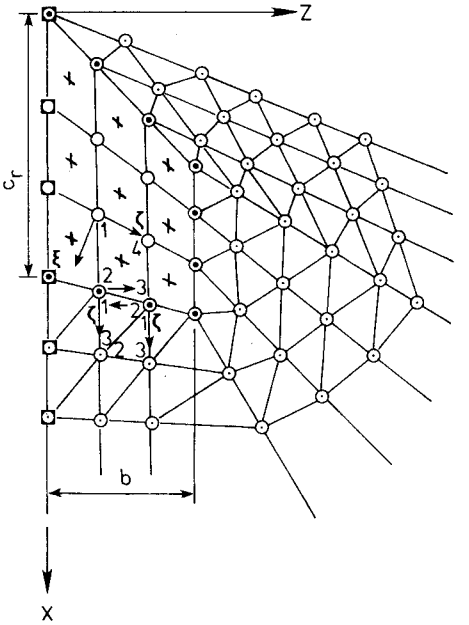

Fig. 2 Arrangement of the bound- and free-vortex panels.

The remaining boundary condition, Eqs. (11-14), are enforced at certain nodes of the vortex panels to obtain the undetermined coefficients of the local vorticity distribution and the shape of the free-vortex panels. The Kutta condition, Eq. (14), is enforced at the nodes of the bound-vortex panels along the edges of separation. The no-penetration condition, Eq. (11), is enforced at the average points of the bound-vortex panels. The no-penetration and no-pressure-jump conditions, Eqs. (12) and (13), are simultaneously satisfied at the nodes of the free-vortex panels.

To satisfy these conditions, an iterative technique is followed which alternately yields the local vorticity distribution on the bound-vortex panels and the shape of the free-vortex panels. During a typical iterative cycle, an overdetermined set of algebraic equations is solved for the undetermined coefficients of the local vorticity distributions. This is followed by adjusting the surface w such that $\bar{\omega}$ and $(\bar{e}_\infty + \nabla\phi)$ at the nodes of the free-vortex panels become parallel. The overdetermined set of equations consists of the equations obtained from the continuity of vorticity condition, Kutta condition, the no-penetration condition on the wing, and a symmetry condition applied at the nodes along the line of symmetry. This set is solved by a least-square technique.

Once the iterative technique converges, the pressure distribution is calculated and this is followed by calculating the total aerodynamic characteristics. Convergence of the technique is expedited by using an initial guess for w provided by the NDV method.[4-6]

In the next subsections, the basic equations required at each step of the solution are given.

Quadrilateral Panel

Planar quadrilateral vortex panels are used to represent the bound-vortex sheet. On each panel, a local linear vorticity distribution is specified. For the kth panel, the vorticity distribution is given by

$$\omega_\zeta(k) = a_1(k) + a_2(k)\zeta(k) + a_3(k)\xi(k) \tag{16}$$

$$\omega_\xi(k) = -a_2(k)\xi(k) - a_4(k) - a_5(k)\zeta(k) \tag{17}$$

which contain five undetermined coefficients a_1-a_5. It should be noted that a linear vorticity distriubiton is equivalent to a quadratic doublet distribution. Within a panel, the distributions given by Eqs. (16) and (17) satisfy the solenoidal property of $\bar{\omega}$.

$$\nabla \cdot \bar{\omega} = 0 \tag{18}$$

The four corners of the panel serve as nodal points where continuity of vorticity condition, Kutta condition, and/or symmetry condition are satisfied. The ζ and ξ axes are located in the panel plane such that the ζ axis coincides with the 1-4 side of the panel. The η axis is perpendicular to the panel such that ζ, ξ, and η axes form a right-handed local coordinate system. The average point of the four nodes serves as the control point where the no-penetration condition is enforced, see Fig. 3a.

In the near field, the induced velocity at any field point, $\hat{x},\hat{y},\hat{z}$, is calculated by

$$\bar{v}(\hat{x},\hat{y},\hat{z}) = \frac{-1}{4\pi}\sum_{i=1}^{2}\left[\int_{\xi_{in}}^{\xi_{fn}}\int_{\zeta_{in}}^{\zeta_{fn}} \times \frac{\hat{y}\omega_\xi\bar{e}_\xi + [(\hat{z}-\zeta)\omega_\xi - (\hat{x}-\xi)\omega_\zeta]\bar{e}_\eta - \hat{y}\omega_\xi\bar{e}_\zeta}{[(\hat{x}-\xi)^2 + \hat{y}^2 + (\hat{z}-\zeta)^2]^{3/2}}\right] d\zeta d\xi \tag{19}$$

where the summation over i indicates that the panel may be divided into two subpanels (in the case of general quadrilateral panel, see Fig. 3a). Substituting Eqs. (16) and (17) into Eq. (19) and integrating, we obtained a closed-form expression for the induced velocity.

In the far field, the vorticity distribution is lumped into concentrated vortex lines and the simpler Biot-Savart law is used to calculate the induced velocity.

Triangular Panels

Planar triangular panels model nonplanar and twisted surfaces more accurately than quadrilateral planar panels. Therefore, they are used to represent the free-vortex sheets where highly nonplanar and twisted surfaces are encountered. The local vorticity distributions are still given by Eqs. (16) and (17). The corners of this panel serve as nodal points where certain boundary conditions are enforced. The ζ axis coincides with the 1-3 side of the panel, the ξ axis is in the panel plane, and the η axis is perpendicular to the panel such that ζ, ξ, and η axes form a righ-handed local coordinate system (Fig. 3b).

In the near field, the induced velocity at any point is given by Eq. (19), where $i=1$. In the far field, the vorticity distribution on the panel is lumped into concentrated vortex lines so that Biot-Savart's law can be used to calculate the induced velocity.

Boundary Conditions

At each control point of the bound-vortex panels, we satisfy Eq. (11). For the mth control point (a receiver panel), Eq. (11) gives

$$\sum_{k=1}^{N}\bar{v}(m,k)\cdot\bar{n}_s(m) = -\bar{e}_\infty\cdot\bar{n}_s(m) \tag{20}$$

where N is the total number of bound- and free-vortex panels (k refers to a sender panel), and

$$\bar{v}(m,k) = \sum_{j=1}^{5}[\tilde{u}_j(m,k)\bar{e}_\xi(k) + \tilde{v}_j(m,k)\bar{e}_\eta(k) + \tilde{w}_j(m,k)\bar{e}_\zeta(k)]a_j(m,k) \tag{21}$$

where $\tilde{u}_j$, $\tilde{v}_j$, and $\tilde{w}_j$ are the velocity components per unit a_j. It should be noted that when $m=k$ the result of Eq. (19) is evaluated at a very small distance from the panel (10^{-6}).

The unit normal $\bar{n}_s(m)$ of a bound-vortex panel and the base unit vectors $\bar{e}_\xi(k)$, $\bar{e}_\eta(k)$, and $\bar{e}_\zeta(k)$ of the local coordinates of the kth sender panel (bound or free) are expressed in terms of the base unit vectors of the global wing-fixed coordinate system $\bar{i}$, $\bar{j}$, and $\bar{k}$ as follows:

$$\bar{n}_s(m) = d_{nx}(m)\bar{i} + d_{ny}(m)\bar{j} + d_{nz}(m)\bar{k} \tag{22}$$

$$\bar{e}_\xi(k) = d_{\xi x}(k)\bar{i} + d_{\xi y}(k)\bar{j} + d_{\xi z}(k)\bar{k}$$

$$\bar{e}_\eta(k) = d_{\eta x}(k)\bar{i} + d_{\eta y}(k)\bar{j} + d_{\eta z}(k)\bar{k}$$

$$\bar{e}_\zeta(k) = d_{\zeta x}(k)\bar{i} + d_{\zeta y}(k)j + d_{\zeta z}(k)\bar{k} \tag{23}$$

where d refers to the direction cosine.

Substituting Eq. (23) into Eq. (21) and substituting the resulting equation and Eq. (22) into Eq. (20), the no-

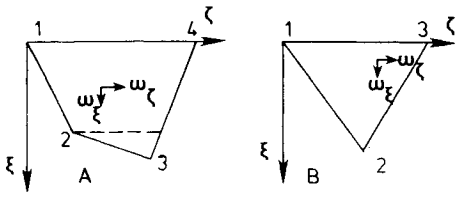

Fig. 3 Quadrilateral and triangular vortex panels.

penetration at any mth point reduces to

$$\sum_{k=1}^{N}\sum_{j=1}^{5}\begin{Bmatrix} d_{nx} \\ d_{ny} \\ d_{nz} \end{Bmatrix}_m^T \begin{bmatrix} d_{\xi x} & d_{\eta x} & d_{\zeta x} \\ d_{\xi y} & d_{\eta y} & d_{\zeta y} \\ d_{\xi z} & d_{\eta z} & d_{\zeta z} \end{bmatrix}_k \begin{Bmatrix} \tilde{u}_j \\ \tilde{v}_j \\ \tilde{w}_j \end{Bmatrix}_{m,k}$$

$$\times a(j,k) = -\begin{Bmatrix} \cos\alpha \\ -\sin\alpha \\ 0 \end{Bmatrix}^T \begin{Bmatrix} d_{nx} \\ d_{ny} \\ d_{nz} \end{Bmatrix}_m \tag{24}$$

It should be noted here that the number of unknown coefficients $a(j,k)$ are reduced from $5N$ ($5\times$total number of bound- and free-vortex panels) to $5N_b$ ($5\times$total number of bound-vortex panels) by equating the outflow of vorticity from the bound-vortex panels to the inflow of vorticity into the free-vortex panels along the separation edges. Moreover, the vorticity vector is aligned with one side of the triangular free-vortex panels. Once this is accomplished, the free argument m has the range 1-N_b and thus we obtain N_b unknowns.

In addition, we write equations of vorticity continuity at each common node of the bound-vortex panels. A typical set of equations written at the $(I+1, j)$ global node, corresponding to the two local nodes $(2,k)$ and $(1,k+1)$ between panels number k and $k+1$, is given by (see Fig. 4)

$$\begin{aligned}
\omega_z(I+1,J) &= \omega_\zeta(2,k)\,d_{\zeta z}(k) + \omega_\xi(w,k)\,d_{\xi z}(k) \\
&= \omega_\zeta(1,k+1)\,d_{\zeta z}(k+1) + \omega_\xi(2,k+1)\,d_{\xi z}(k+1) \\
\omega_x(I+1,J) &= \omega_\zeta(2,k)\,d_{\zeta x}(k) + \omega_\xi(2,k)\,d_{\xi x}(k) \\
&= \omega_\zeta(1,k+1)\,d_{\zeta x}(k+1) + \omega_\xi(1,k+1)\,d_{\xi x}(k+1)
\end{aligned} \tag{25}$$

where ω_ξ and ω_ζ are expressed in terms of the undetermined coefficients $a(j,k)$ using Eqs. (16) and (17).

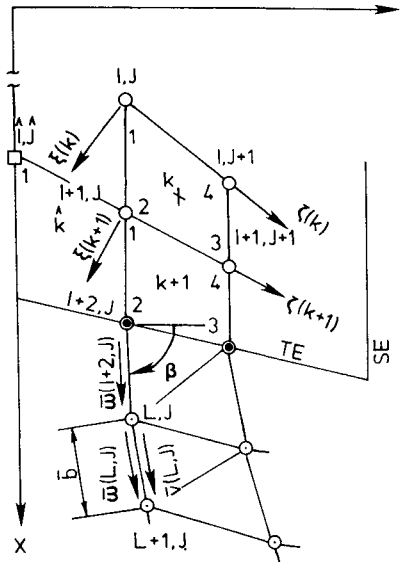

+ No-Penetration Condition
O Continuity of Vorticity Condition
• Kutta Condition
□ Symmetry Condition
Kinematic and Dynamic Conditions

Fig. 4 Details of the boundary conditions and control points.

The Kutta condition, Eq. (14), is satisfied at the nodes of bound-vortex panels along the edges of separation. At a typical global node $(I+2,J)$, Eq. (14) gives

$$\omega_x(I+2,J)\,v_z(I+2,J) - \omega_z(I+2,J)\,v_x(I+2,J) = 0 \tag{26}$$

Since ω_x, ω_z, v_x, and v_z are functions of the undetermined coefficients, Eq. (26) is a nonlinear equation in $a(j,k)$. Adding equations of this type to Eqs. (24) and (26) disturbs the linearity of the resulting set of equations. Therefore, we divide Eq. (26) by $v(I+2,J)$ to obtain

$$\omega_x(I+2,J)\cos\beta(I+2,J) - \omega_z(I+2,J)\sin\beta(I+2,J) = 0 \tag{27}$$

where $\beta(I+2,J)$ is the angle of $\bar{v}(I+2,J)$ with the x axis. Assuming that $\beta(I+2,J)$ is initially kown, Eq. (27) becomes a linear equation in the a coefficents. In the subsequent iterative steps, the angle β is calculated using the a values of the preceding iterative step.

The last set of linear equations is obtained from the symmetry condition (for symmetric flow) along the root chord. A typical symmetry condition written at a global node $(\hat{I},\hat{J})$, corresponding to a local note $(1,\hat{k})$, is given by

$$\omega_x(\hat{I},\hat{J}) = \omega_\zeta(1,\hat{k})\,d_{\zeta x}(\hat{k}) + \omega_\xi(1,\hat{k})\,d_{\xi x}(\hat{k}) = 0 \tag{28}$$

The resulting set of equations obtained from Eqs. (24), (25), (27), and (28) is solved for the coefficients a by a least-square solver (overdetermined set of equations).

Once the coefficients are determined, Eqs. (12) and (13) are enforced by aligning sides 1-3 of the triangular free-vortex panels with the local flow directions. Equations of the following form are used to calculate the new global downstream nodes of these sides:

$$\begin{aligned}
x(L+1,J) &= x(L,J) + \tilde{b}v_{mx}(L,J)/v_m(L,J) \\
y(L+1,J) &= y(L,J) + \tilde{b}v_{my}(L,J)/v_m(L,J) \\
z(L+1,J) &= z(L,J) + \tilde{b}v_{mz}(L,J)/v_m(L,J)
\end{aligned} \tag{29}$$

where (L,J) and $(L+1,J)$ refer to the upstream and downstream nodes of side 1-3, $\tilde{b}$ is the length of this side, and v_m the velocity calculated at the upstream node (L,J).

Pressure Distribution

The net pressure distribution is calculated at the no-penetration control point of a bound-vortex panel. At the mth control point, the net pressure coefficient is given by

$$\Delta C_p(m) = 2\left\{\omega_x(m)\sum_{k=1}^{N} v_z(m,k) - \omega_z(m)\left[\sum_{k=1}^{N} v_x(m,k) + \cos\alpha\right]\right\} \tag{30}$$

where

$$\begin{aligned}
\omega_x(m) &= \omega_\zeta(m)\,d_{\zeta x}(m) + \omega_\xi(m)\,d_{\xi x}(m) \\
\omega_z(m) &= \omega_\zeta(m)\,d_{\zeta z}(m) + \omega_\xi(m)\,d_{\xi z}(m)
\end{aligned} \tag{31}$$

The normal force coefficient is then calculated by

$$C_n = \sum_{m=1}^{N_b} \Delta C_p(m)\,A(m) \Big/ \sum_{m=1}^{N_b} A(m) \tag{32}$$

where $A(m)$ is the area of mth panel.

IV. Nonlinear Hybrid Vortex Method for Unsteady Flows

A. Governing Equations

For unsteady symmetric flow, we set $\beta=\gamma=\dot{\beta}=\dot{\gamma}=0$ in Eqs. (1) and (2). The resulting equations are

$$\bar{e}_\infty=\cos\alpha\bar{i}-\sin\alpha\bar{j} \tag{33}$$

$$\bar{\Omega}=\Omega_z\bar{k}=\dot{\alpha}\bar{k} \tag{34}$$

$$\nabla^2\phi=0 \tag{35}$$

$$(\bar{e}_\infty+\nabla\phi-\bar{\Omega}_z\times\bar{r})\cdot\bar{n}_s=0 \qquad \text{on } s(\bar{r})=0 \tag{36}$$

$$\partial w/\partial t+(\bar{e}_\infty+\nabla\phi-\bar{\Omega}_z\times\bar{r})\cdot\nabla w=0 \qquad \text{on } w(\bar{r},t)=0 \tag{37}$$

$$D\Gamma/Dt=0 \qquad \text{on } w(\bar{r},t)=0 \tag{38}$$

$$\Delta C_p\,|_{\text{TE,LE,SE}}=0 \tag{39}$$

$$\nabla\phi\to 0 \qquad \text{away from } s \text{ and } w \tag{40}$$

B. Method of Solution of the Unsteady Flow Problem

The source of flow unsteadiness in this problem can be a time-dependent angle of attack or a time-dependent free-stream speed. In the time-domain approach of this problem we divide the function of angle of attack into discrete changes in the angle of attack corresponding to discrete changes in teime, i.e., at $t=t_0$, $\alpha=\alpha_0$ and at $t=t_0+\Delta t$, $\alpha=\alpha_0+\Delta\alpha$, etc. The problem is then solved at each time step where the solution of the preceding time step serves as the initial condition for the present time step.

This approach can treat problems where the flow unsteadiness starts (at $t=t_0$) from a steady flow or where the flow unsteadiness starts impulsively from rest. The former problem initially requires the steady flow solution to be known, while the latter problem initially requires the solution of the flow over a wing without a wake surface.

Once the intial condition is obtained, we march step by step in time satisfying Eqs. (36-39). At each time step, the basic unknowns $\bar{\omega}(\bar{r},t)$ and $w(\bar{r},t)$ are obtained.

Next, we discuss the boundary conditions and the calculations of the pressure distribution at each step.

Boundary Conditions

Although the developed time-domain technique is a general one and moreover is not restricted to any particular source of flow unsteadiness, the case of an impulsively started wing from rest is considered for the purpose of explaining the details of the technique. In this case, we set $\alpha=0$ and replace $\bar{e}_\infty$ by $-\bar{e}_\infty$ in Eqs. (33), (34), (36), and (39).

1) The initial condition, at $t=t_0$, is considered to be a wing without a wake surface having a velocity of $-\bar{e}_\infty$. At this instant, we assume that not enough time has passed for the vorticity to be convected from the separation edges. The initial vorticity distribution of the wing $\bar{\omega}(\bar{r},t)$ is obtained from the least-square solution of an overdetermined set of linear algebraic equations in the unknown coefficients a [Eqs. (36), (25), (39), (28)].

It should be noted that the initial vorticity distribution on the wing is such that the circulation around any closed curve embracing a wing section or equivalently the outflow of vorticity from a surface enclosed by this curve is zero. Consequently, a starting vortex of opposite strength to that of the vorticity on the wing develops at the edges of separation. The starting vortex is then convected downstream with the local particle velocity, the flow existing at the preceding instant is disturbed, and the vorticity distribution on the wing changes creating a new starting vortex.

This process continues and by the end of the first time step, at $t=t_0+\Delta t$, a free-vortex strip, consisting of triangular free-vortex panels attached to the separation edges, is created. The free-vortex strip obeys the conditions given by Eqs. (37) and (38) and its upstream edge satisfies the Kutta condition at the separation edges, Eq. (39).

2) At $t=t_0+\Delta t$, one needs $\bar{v}(\bar{r},t_0+\Delta t)$ to determine the width of the vortex strip. Since this velocity is unknown so far, a good estimate is taken as the velocity at the preceding time step $\bar{v}(r,t_0)$, which is completely known from the solution corresponding to the initial condition. Within the time step Δt, the displacement $\Delta\bar{r}$ of any panel node is found from

$$\Delta\bar{r}=\bar{r}(t_0+\Delta t)-\bar{r}(t_0)=\Delta t\cdot\bar{v}(\bar{r},t_0) \tag{41}$$

where

$$\bar{v}(\bar{r},t_0)=-\bar{e}_\infty+\nabla\phi(\bar{r},t_0)$$

At $t=t_0+\Delta t$, one also needs the vorticity of the triangular vortex panels forming the free-vortex strip, $\bar{\omega}_w(\bar{r},t_0+\Delta t)$. For each triangular panel, we express its five unknown coefficients (a_1-a_5), describing its linear vorticity distribution, in terms of the five unknown coefficients of the adjacent bound-vortex panel, at the separation edges, at $t=t_0$ (a_1-a_5 of the bound panel are already known) and at $t=t_0+\Delta t$ (a_1-a_5 of the bound panel are still unknown). This is achieved by satisfying the continuity of vorticity at the global nodes on the

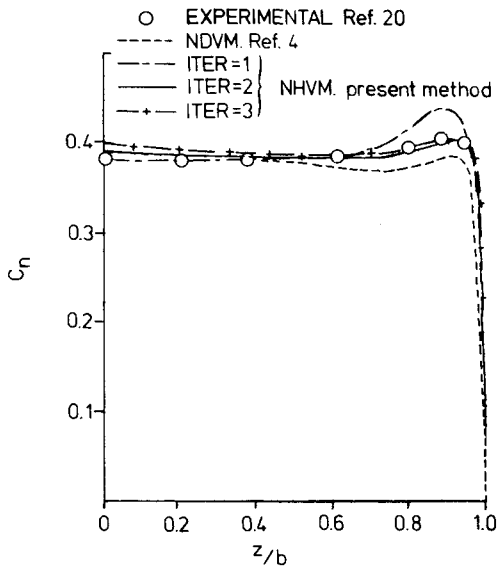

Fig. 5 Spanwise variation of normal-force coefficient, $\mathcal{R}=1$, $\alpha=9.7$ deg, 6×6 bound panels.

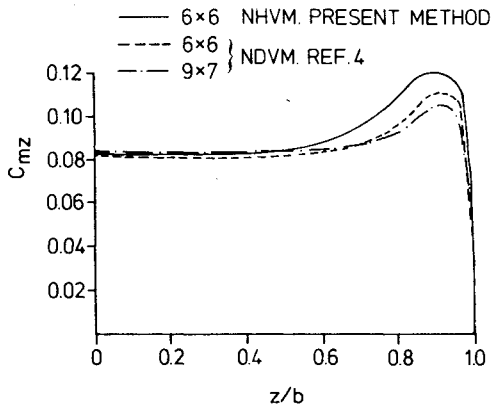

Fig. 6 Spanwise variation of pitching-moment coefficient, $\mathcal{R}=1$, $\alpha=9.7$ deg.

separation edges and Kelvin theorem, Eq. (36), between $t=t_0$ and $t=t_0+\Delta t$.

Next, the vorticity distribution on the wing $\bar{\omega}(r,t_0+\Delta t)$ is obtained from the overdetermined set of algebraic equations.

3) At $t=t_0+2\Delta t$, a new free-vortex strip is created along the separation edges, the first shed free-vortex strip is convected downstream under the condition $D\Gamma/Dt=0$, and step 2 is repeated to find the locations of the free-panel nodes and $\bar{\omega}(r,t_0+2\Delta t)$.

4) The steady state is reached once the change in the vorticity distribution is less than a prescribed error.

Pressure Distribution

To calculate the net pressure coefficient at any point on the wing surface $\bar{r}$ at any time $t_k=t_0+k\cdot\Delta t$, we apply the unsteady Bernoulli equation

$$\Delta C_p(\bar{r},t_k)=-2\bar{V}_j(\bar{r},t_k)\cdot[\nabla\phi(\bar{r},t_k)+(\bar{e}_\infty-\bar{\alpha}\bar{k}\times\bar{r})]-2\frac{\partial\Delta\phi(\bar{r},t_k)}{\partial t} \tag{42}$$

where $\bar{V}_j(\bar{r},t_k)$ is the jump in the tangential velocity across the wing, which is completely known from the vorticity vector at this location, $\bar{\omega}(\bar{r},t_k)$. The first term in the brackets $\nabla\phi(\bar{r},t_k)$ is calculated from Eq. (19). The last term on the right-hand side is calculated as follows:

$$\frac{\partial\Delta\phi(\bar{r},t_k)}{\partial t}=\frac{\Delta\phi(\bar{r},t_k)-\Delta\phi(\bar{r},t_{k-1})}{\Delta t}=\frac{\Gamma(\bar{r},t_k)-\Gamma(\bar{r},t_{k-1})}{\Delta t} \tag{43}$$

V. Computer Program

A computer program is developed to implement the methods of solution of the steady and unsteady flow problems. The program is divided into three major parts and each part consists of several subroutines.

The first part deals with the wing geometry, wing paneling (bound-vortex panels), and wake paneling (free-vortex panels). Usage of initial wake paneling depends on the initial conditions of the unsteady problem. No wake paneling is considered if the unsteady problem starts from rest. For the unsteady problem with steady-state initial condition, wake paneling is considered.

The second part deals with initial conditions. For the unsteady problem with steady-state initial conditions, the steady flow problem is initially solved. The boundary conditions on the bound- and free-vortex panels are satisfied through several subroutines. Once the boundary conditions are satisfied, the net pressure coefficients are calculated. If the initial condition is rest, the problem is solved without any free-vortex panels.

The third part of the program deals with the problem at $t>t_0$. Several subroutines are used to satisfy the boundary conditions at the subsequent time steps $t_k=t_0+k\cdot\Delta t$; $k=1,2,\ldots$. One subroutine is used to generate a new shed free-vortex strip and another subroutine is used to convect the previously shed free-vortex strips. The vorticity distribution of the panels forming the previously shed free-vortex strips $\bar{\omega}_w(\bar{r},t_k)$ is found from another subroutine which enforces Kelvin theorem. The unknown vorticity coefficients of the panels forming the newly shed vortex-sheet strip are related to those coefficients of the wing panels existing at the separation edges.

Other subroutines are used to fill the matrix representing the wing boundary conditions; no-penetration condition, continuity of vorticity condition, unsteady Kutta condition, and symmetry condition. The least-square solver is used to obtain the vorticity distribution at this time step, $\bar{\omega}(\bar{r},t_k)$.

The unsteady Bernoulli equation is then used through a separate subroutine to calculate the net pressure coefficient.

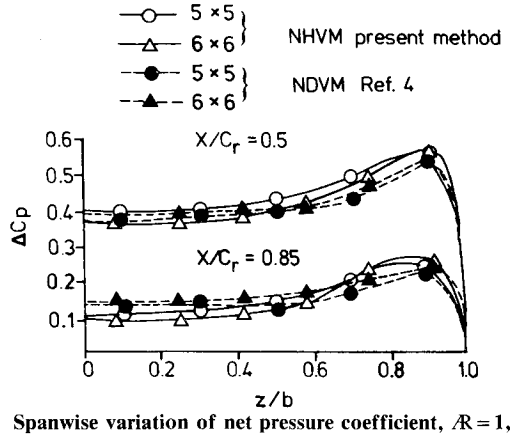

Fig. 7 Spanwise variation of net pressure coefficient, $\mathcal{R}=1$, $\alpha=15$ deg.

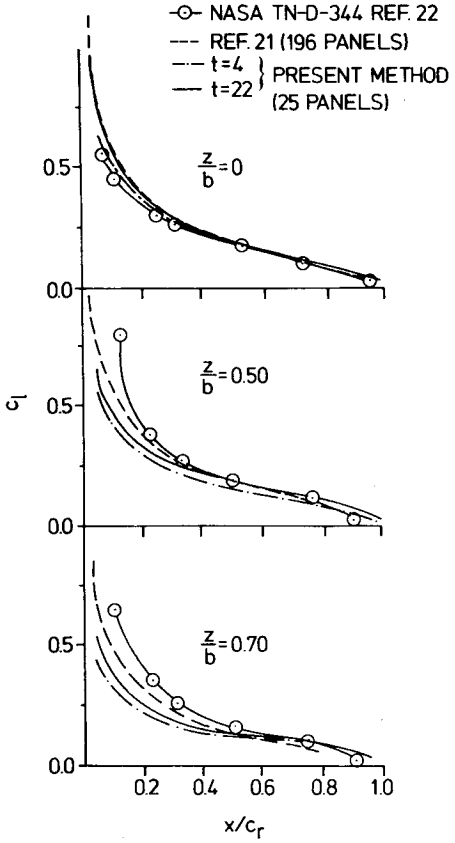

Fig. 8 Chordwise variation of the lift coefficient, $\mathcal{R}=3$, $\alpha=5$ deg, 5×5 bound panel, no tip separation.

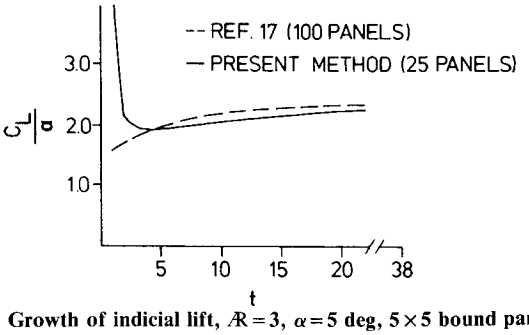

Fig. 9 Growth of indicial lift, $\mathcal{R}=3$, $\alpha=5$ deg, 5×5 bound panels, no tip separation.

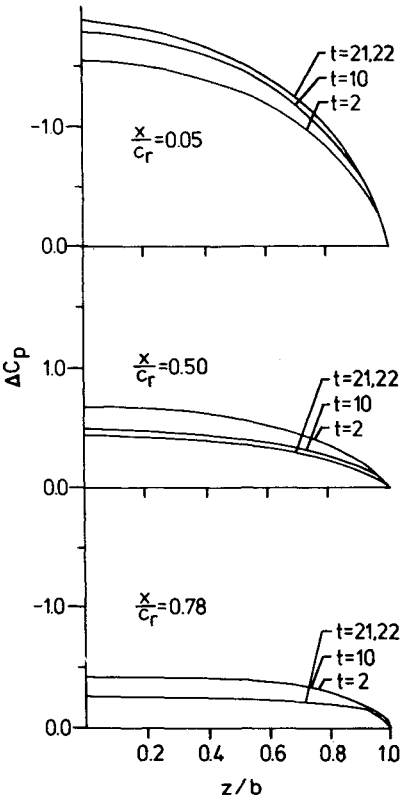

Fig. 10 Spanwise variation of net pressure coefficient, $\mathcal{R}=2$, $\alpha=20.5$ deg, 5×5 bound panels, no tip separation.

VI. Numerical Examples

A. Steady Flow

The developed computer program is used to solve for the steady flow past a rectangular wing having side-edge separation. The wing is of aspect ratio of 1 at 9.7 deg angle of attack. The wing is divided into 6×6 quadrilateral bound-vortex panels, the trailing-edge free-vortex sheet is divided into 6×6 quadrilateral free-vortex panels, and the side-edge free-vortex sheet is divided into six vortex strips, and each is divided into a different number of quadrilateral free-vortex panels such that the last panel in each strip occupies the same chordwise station as that of the last panel of the trailing-edge free-vortex panel.

Figure 5 shows the spanwise variation of the section normal-force coefficient at three iteration steps. The solution converges in the third iteration step and is in good agreement with the experimental data of Scholtz.[18] The figure also shows the solution of the same case obtained by the NDV method with 6×6 bound-vortex lines. One can conclude that the NDV method underestimates the normal-force coefficient near the wing tip. If the number of bound-vortex lines of the NDV method is increased to 9×7^4, the solution agrees with that obtained by the NHV method with 6×6 bound-vortex panels.

This clearly shows that a small number of vortex panels gives the same accuracy as that obtained by a large number of bound-vortex lines.

Figure 6 shows the converged solution of the spanwise variation of the section pitching-moment coefficient for the wing. The results of the NDV method with 6×6 and 9×7 bound-vortex lines are also included in the figure.

Figure 7 shows the spanwise variation of the net pressure coefficient at different chord stations with a different number of panels for a rectangular wing at 15 deg angle of attack. The corresponding results of the NDV method are also shown in the figure.

The present computer program is computationally efficient. The CPU time on the CYBER 175 for this case is about 200 s.

B. Unsteady Flow

Next, the developed computer program is used to solve for the unsteady flow past impulsively started wings from rest without side-edge separation. In the two examples, the wing is divided into 5×5 quadrilateral bound-vortex panels with a sine distribution in the chordwise direction and a cosine distribution in the spanwise direction. In the present cases, the dimensionless time step is equivalent to 0.48 while the root-chord length is 5 units.

Figure 8 shows the distribution of the lift coefficient for a rectangular wing of aspect ratio of 3 at 5 deg angle of attack for $t=2$ and 22. The present results are compared with the steady numerical data of Ref. 19 where 196 panels of constant potential function are used. It is also compared with the experimental data of Ref. 20. Although we used 25 panels in the present case, the results compare well with the other numerical and experimental data.

Figure 9 compares the growth of indicial lift for the same wing considered above with the numerical data of Ref. 17 where 100 panels of constant doublets are used.

Figure 10 shows the distribution of net pressure coefficient for a rectangular wing of aspect ratio 2 at 20.5 deg angle of attack for $t=2$, 10, 21, and 22. On the CYBER 175 computer, the CPU time for each case with 5×5 bound panels and 22 time steps is about 10 min.

Currently, work is underway to calculate cases with side- and leading-edge separations.

VII. Concluding Remarks

A steady and unsteady nonlinear hybrid vortex (NHV) method for low aspect ratio wings at large angles of attack in incompressible flow is developed. The method uses vortex panels with linear vorticity distribution (equivalent to quadratic doublet distribution) in the near field calculations. In the far field, the distribution vorticity is reduced to concentrated vortex lines where the simpler Biot-Savart law is employed for the velocity field calculations. The method is applied to steady and unsteady flow problems without any restrictions on the order of magnitude of the disturbances in the flowfield. The presented numerical results show that the method produces accurate results and it is computationally efficient.

Acknowledgments

This work has been supported by NASA Langley Research Center, Hampton, Va., under Grant NSG-1560 with Dr. E. Carson Yates Jr. as the technical monitor; and by the Naval Air Development Center in Warminister, Pa., under Contract N 62269-80-C-0704 with Mr. Marvin Walters as the technical monitor.

References

[1] Belotserkovskii, S. M., "Calculations of the Flow Around Wings of Arbitrary Planforms Over a Wide Range of Angles of Attack," NASA TT F-12, 391, 1969.

[2] Rehbach, C., "Calculation of Flow Around Zero-Thickness Wings with Evolute Vortex Sheets," NASA TT F-15,183, 1973.

[3] Rehbach, C., "Numerical Investigation of Vortex Sheets Issuing from Separation Line Near the Leading Edge," NASA TT F-15,530, 1974.

[4] Kandil, O. A., Mook, D. T., and Nayfeh, A. H., "Nonlinear Prediction of the Aerodynamic Loads on Lifting Surfaces," *Journal of Aircraft*, Vol. 13, Jan. 1976, pp. 22-28.

[5] Kandil, O. A., "Numerical Prediction of Vortex Cores from the Leading and Trailing Edges of Delta Wings," ICAS Paper 14.2, The 12th Congress of the International Council of the Aeronautical Sciences, Munich, FRG, Oct. 1980.

[6]Kandil, O. A. and Balakrishnan, L., "Recent Improvements in the Prediction of the Leading and Trailing Edge Vortex Cores of the Delta Wings," AIAA Paper 81-1263, 1981.

[7]Johnson, R. T. and Rubbert, P. E., "Advanced Panel-Type Influence Coefficient Methods Applied to Subsonic Flows," AIAA Paper 75-50, 1975.

[8]Weber, J. A., Brune, G. W., Johnson, F. T., Lu, P., and Rubbert, P. E., "Three Dimensional Solution of Flows Over Wings with Leading Edge Vortex Separation," *AIAA Journal*, Vol. 14, 1976, pp. 519-525.

[9]Johnson, F. T., Tinoco, E. N., Lu, P., and Epton, M. A., "Recent Advances in the Solution of Three-Dimensional Flows over Wings with Leading Edge Vortex Separation," AIAA Paper 79-0282, 1979.

[10]Kandil, O. A., Chu, L., and Yates, E. C. Jr., "Hybrid Vortex-Method for Lifting Surfaces with Free Vortex Flow," AIAA Paper 80-0070, 1980.

[11]Chu, L., "Nonlinear Hybrid-Vortex Method for Wings Having Side-Edge Separations," M.S. Thesis, Old Dominion University, Norfolk, Va., Dec. 1980.

[12]Atta, E. H., Kandil, O. A., Mook, D. T., and Nayfeh, A. H., "Unsteady Aerodynamic Loads on Arbitrary Wings Including Wing-Tip and Leading Edge Separations," AIAA Paper 77-156, 1977.

[13]Kandil, O. A., Atta, E. H., and Nayfeh, A. H., "Three Dimensional Steady and Unsteady Asymmetric Flow Past Wings of Arbitrary Planforms," *Unsteady Aerodynamics*, AGARD CP No. 27, 1978, pp. 2.1-2.19.

[14]Belotserkovskii, S. M. and Nisht, M. I., "Nonstationary Nonlinear Theory of a Thin Wing of Arbitrary Planform," *Mechanika Zhidkosti Gasa*, No. 4, 1974, pp.100-108.

[15]Lavin, D. and Katz, J., "Vortex-Lattice Method for the Calculation of the Nonsteady Separated Flow over Delta Wings," *Journal of Aircraft*, Vol. 18, Dec. 1981, pp. 1032-1037.

[16]Summa, J. M., "Potential Flow About Three-Dimensional Lifting Configurations with Application to Wings and Rotors," AIAA Paper 75-126, 1975.

[17]Summa, J. M., "A Numerical Method for the Exact Calculation of Airloads Associated with Impulsively Started Wings," AIAA Paper 77-002, 1977.

[18]Scholtz, Von N., "Kraft und Druckverteilungsmessumgen an Trägflachen Kleiner Streckung," *Forsharb. Ing. Wes.*, No. 16, 1949, pp. 85-92.

[19]Morino, L. and Tseng, K., "Time-Domain Green's Function Method for Three-Dimensional Nonlinear Subsonic Flows," AIAA Paper 78-1204, 1978.

[20]Lessing, H. C., Troutman, J. C., and Menees, G. P., "Experimental Determination of the Pressure Distribution on a Rectangular Wing Oscillating in the First Bending Mode for Mach Numbers from 0.24 to 1.30," NASA TN D-344, 1960.